

Turnover of Bacterial Cell Wall by SltB3, a Multidomain Lytic Transglycosylase of *Pseudomonas aeruginosa*

Mijoon Lee,[#] Teresa Domínguez-Gil,[§] Dusan Heseck,[#] Kiran V. Mahasenan,[#] Elena Lastochkin,[#] Juan A. Hermoso,^{*§} and Shahriar Mobashery^{*#}

[#]Department of Chemistry and Biochemistry, Nieuwland Science Hall, Notre Dame, Indiana 46556, United States, [§]Department of Crystallography and Structural Biology, Inst. Química-Física “Rocasolano”, CSIC, Serrano 119, 28006 Madrid, Spain

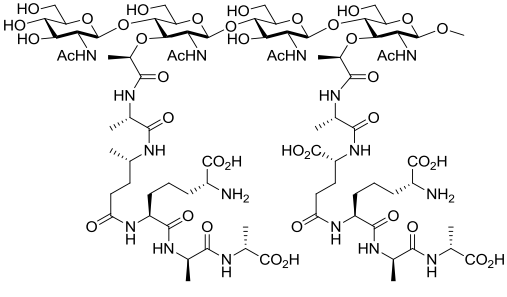
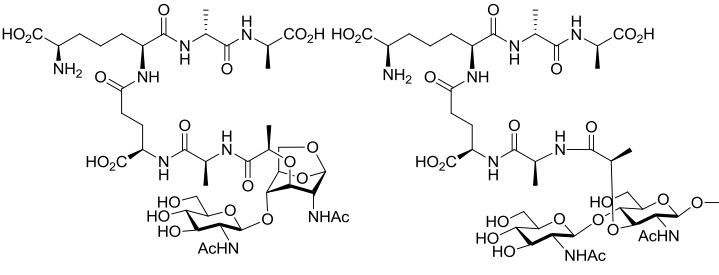
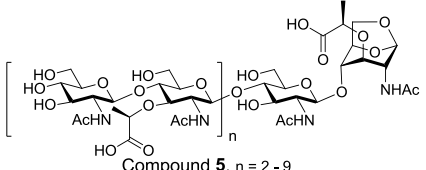
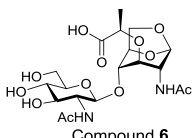
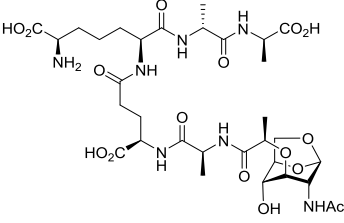
Supporting Information

Contents

Table S1. Compounds used in this study	S2
Figure S1. The protein sequence and SDS-PAGE analysis	
of the purified recombinant SltB3	S3
Figure S2. CID mass spectra of reaction products 1 and 2	S4
Figure S3. Michaelis-Menten plot for turnover of 1 by SltB3	S3
Table S2. Crystallographic data collection and refinement statistics	S5
Figure S4. Structural homologues of SltB3	S6
Figure S5. Electron density maps for compounds 3 and 4	S7
Figure S6. Structural analysis of the interactions found at the core of	
the N-terminal domain.	S8
Figure S7. Structural comparison of active sites of SltB3 and Slt35	
from <i>E. coli</i>	S8
References	S9

Compounds used in this study. Compounds used in this study are given in Table S1. Compounds **1**, **3**, and **4** were prepared according to the synthetic methods that we have published earlier.¹ Compound **5** is a mixture of oligosaccharides with 6-20 sugar moieties, prepared as reported previously.² Compound **9** was the internal standard for kinetic evaluation of turnover of compound **1** to compounds **3** and **4** by SlTB3.

Table S1. Compounds used in this study.

Substrate	Product	
 <p style="text-align: center;">Compound 1</p>	 <p style="text-align: center;">Compound 3 Compound 4</p>	
 <p style="text-align: center;">Compound 5, n = 2 - 9</p>	 <p style="text-align: center;">Compound 6</p>	
Internal standard		
 <p style="text-align: center;">Compound 9</p>		

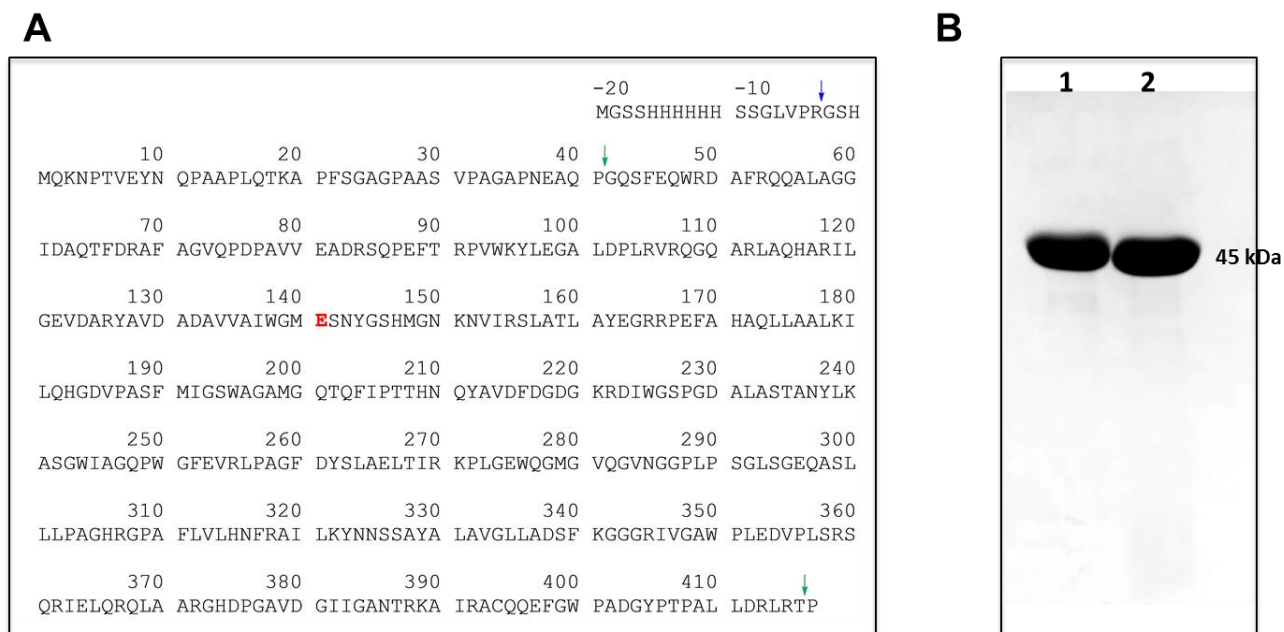


Figure S1. (A) The protein sequence of the recombinant SltB3 used in this study. The thrombin cleavage site is indicated by the blue arrow. The green arrows indicate the beginning and the end of the protein sequence as seen by the X-ray structure. The catalytic Glu141 is given in red. (B) SDS-PAGE analysis of the purified recombinant SltB3 (10 μ g) with His-tag (lane 1) and without His-tag (lane 2).

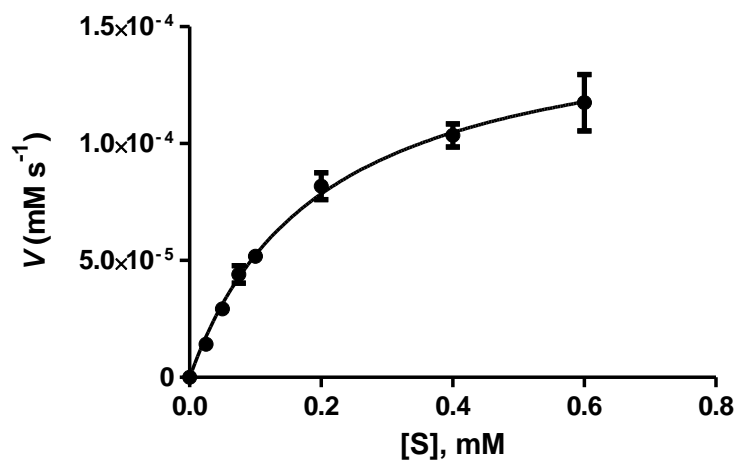


Figure S3. Michaelis-Menten plot for turnover of **1** by SltB3 ([E] = 8 nM).

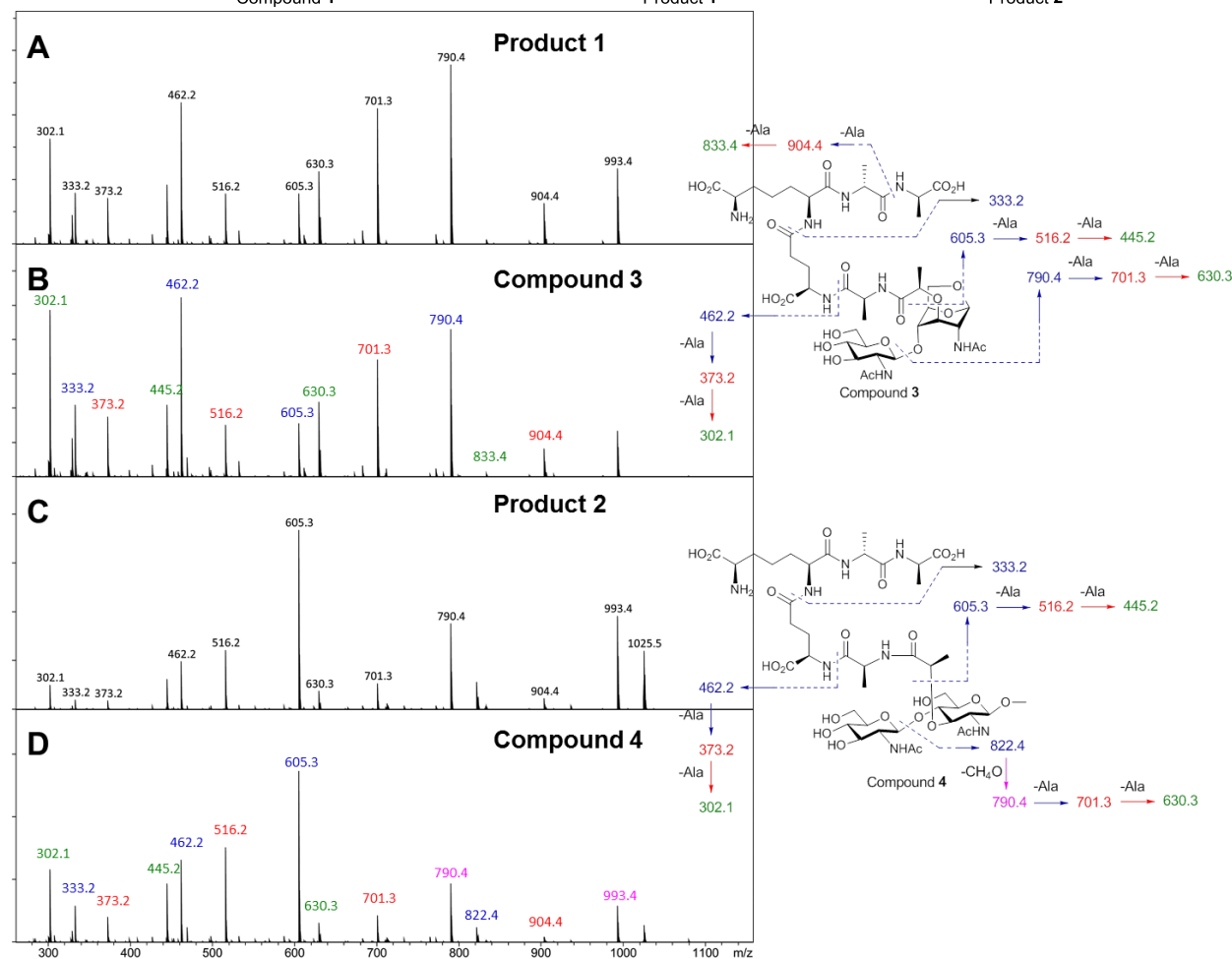
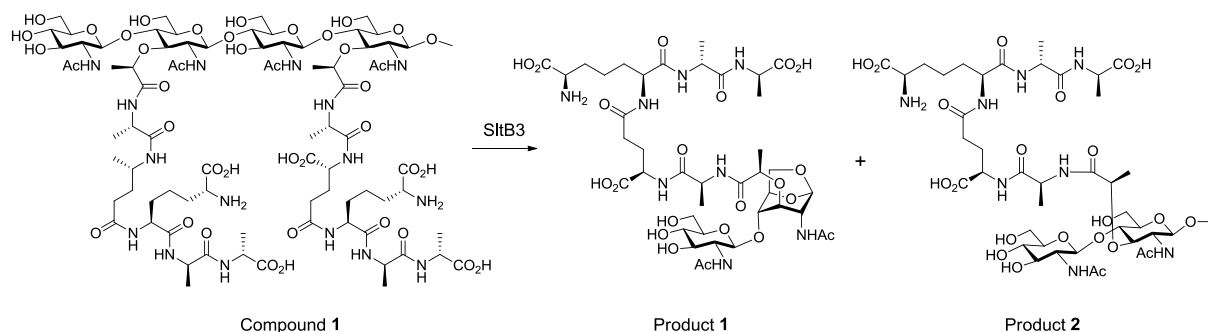


Figure S2. CID mass spectra of product 1 (A), of synthetic standard 3 (B), of product 2 (C), and of synthetic standard 4 (D). Fragmentations of the reaction products 1 and 2 were similar to those of respective synthetic standards (compound 3 for product 1, compound 4 for product 2). Peaks at m/z values in blue, 790.4, 605.3, 462.2 and 333.2 represent the ions formed by the concomitant loss of dehydro NAG, dehydroanhydroNAG, lactate and L-Ala, and *m*-DAP from precursor ion at m/z 993.4 (A and B). Peaks at m/z values in red, 904.4, 701.3, 516.2 and 373.2 represent the ions formed by the concomitant loss of terminal D-Ala (89 Da). Peaks at m/z values in green, 833.4, 630.3, 445.2 and 302.1 represent the ions formed by the concomitant loss of the second D-Ala (71 Da). The peak at m/z 933.4 in C and D represents the ion formed by neutral loss of CH_4O from precursor ion at m/z 1025.5 (and this is chemically identical to compound 3). Hence, the rest of peaks of fragment ions of product 2 (compound 4) are similar to product 1 (compound 3), except the peak at m/z 822.4, formed by concomitant loss of NAG from the precursor ion at m/z 1025.5.

Table S2. Crystallographic data collection and refinement statistics*

	ApoSltB3	SltB3:3 complex	SltB3:4 complex
Diffraction data statistics			
Wavelength (Å)	1.00001	1.05739	0.97626
Space group	P2 ₁ 2 ₁ 2	P2 ₁ 2 ₁ 2	P2 ₁ 2 ₁ 2
<i>a</i> , <i>b</i> , <i>c</i> (Å)	112.28, 61.84, 50.63	111.30, 61.53, 49.94	111.10, 61.44, 49.87
$\alpha=\beta=\gamma$ (°)	90	90	90
Resolution range (Å)	56.14 (1.70- 1.61)	55.65 (1.81-1.77)	61.44 (2.30-2.23)
Unique reflections	46193 (6670)	34168 (1919)	17322 (1581)
Completeness (%)	99.9 (100.0)	99.8 (99.6)	99.9 (99.8)
Redundancy	6.8 (9.1)	12.6 (12.9)	8.5 (8.7)
CC1/2	1.00 (0.93)	1.00 (0.93)	1.00 (0.98)
R _{merge}	0.03 (0.70)	0.09 (0.77)	0.06 (0.36)
R _{pim}	0.01 (0.24)	0.04 (0.31)	0.02 (0.13)
Wilson B-factor (Å ²)	22.1	17.8	29.1
Average I/σ(I)	48.6 (2.7)	20.8 (4.2)	12.3 (4.2)
Refinement statistics			
Resolution range (Å)	54.17-1.61	30.76-1.77	45.56-2.23
R _{work} /R _{free}	0.18/0.20	0.17/0.20	0.18/0.23
No. Atoms	3133	3242	3044
Protein	2900	2881	2876
Water	233	272	68
Ligand	-	89	100
B-factor (Å ²)			
Protein	37.10	27.90	49.10
Water	43.40	38.10	46.80
Ligand	-	49.5	69.5
R.m.s. deviations			
Bond length (Å)	0.006	0.006	0.007
Bond angles (°)	0.99	1.05	1.09
Ramachandran	99/0.0	97/0.2	94/1.8
Favored/outliers (%)			
Monomers per AU	1	1	1
PDB code	5ANZ	5AO7	5AO8

*Values between parentheses correspond to the highest resolution shells

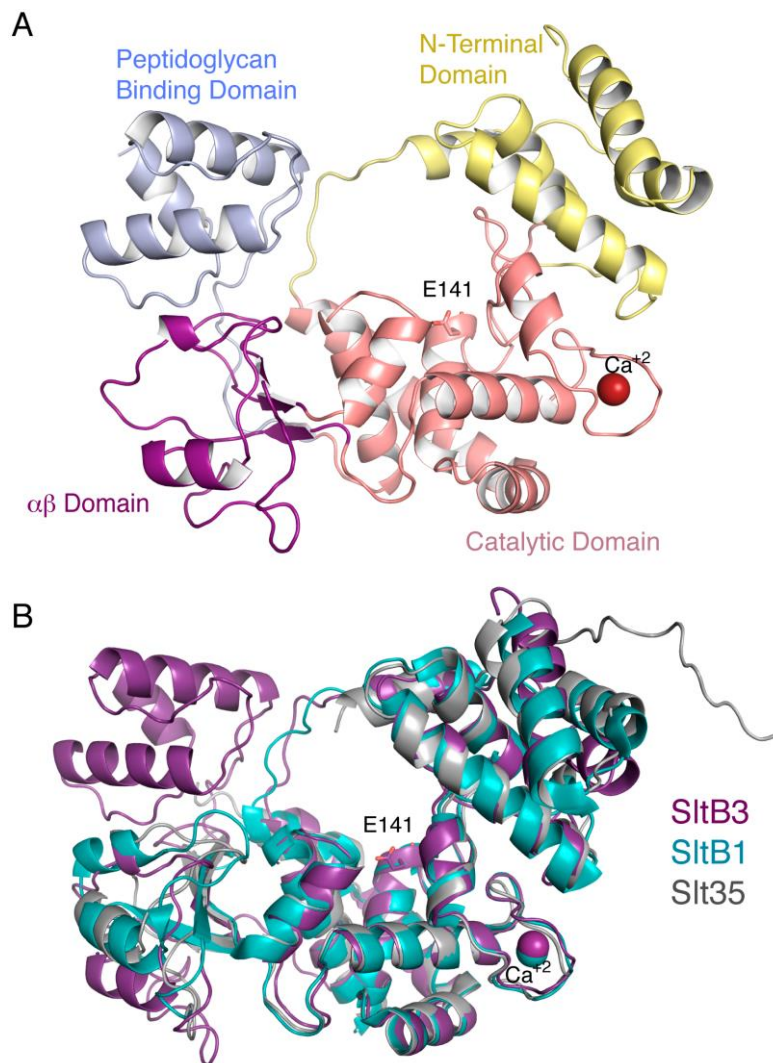


Figure S4. (A) Ribbon representation of the crystal structure of apo SltB3. Each domain is colored differently. N-Terminal domain in yellow, catalytic domain in pink, $\alpha\beta$ domain in magenta and peptidoglycan-binding domain in light blue. The proposed catalytic Glu141 is represented as capped sticks and labeled. Ca cation is represented in spheres (B) Structural comparison of SltB3 with its closest homologues. The closest structural homologues as provided by DALI server³ are the soluble lytic transglycosylases SltB1 from *P. aeruginosa* (PDB 4ANR, rmsd of 1.89 Å over 375 aligned C α atoms) and Slt35 from *E. coli* (PDB 1QUS, rmsd of 2.18 Å over 375 aligned C α atoms).

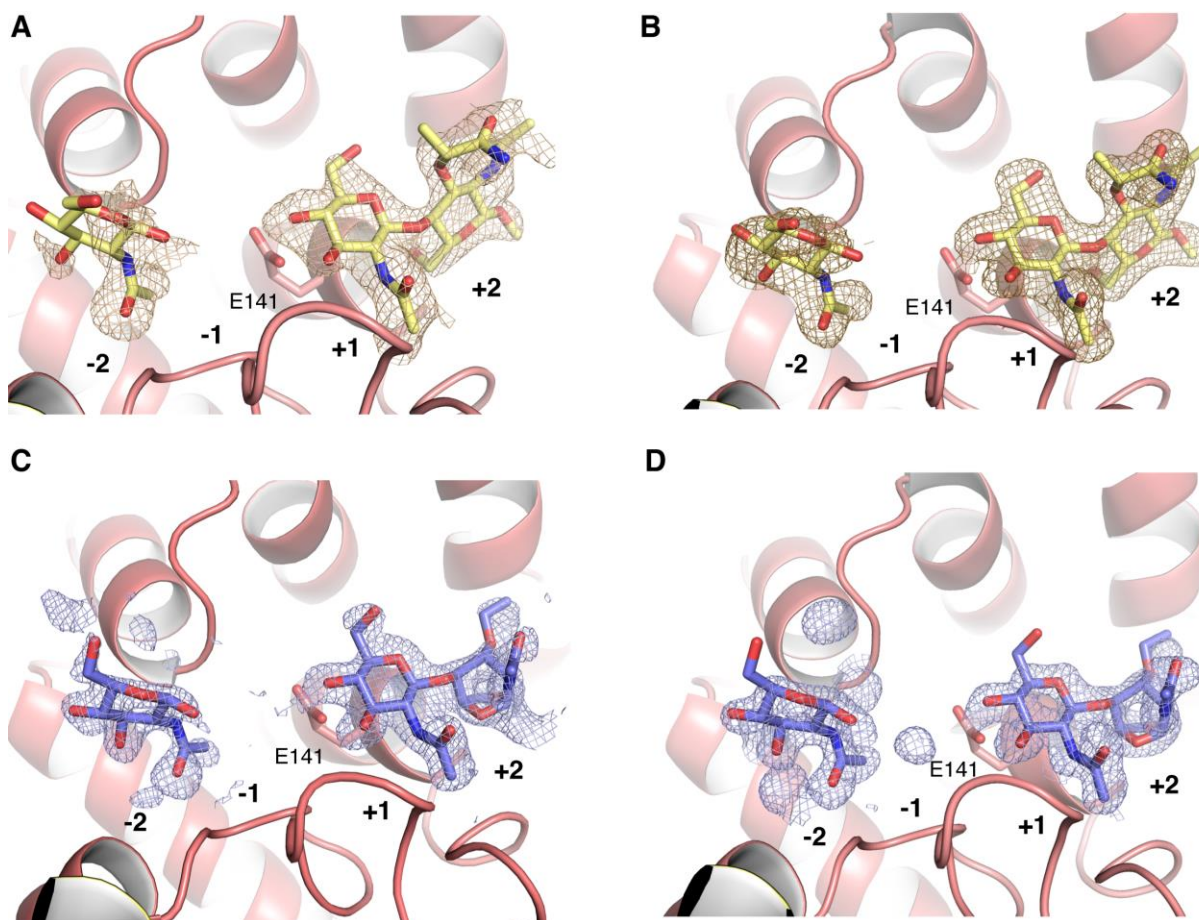


Figure S5. (A) Fo-Fc omit map contoured at 2σ for the two molecules of compound **4** (β -methoxy *N*-acetylglucosamine-*N*-acetylmuramyl L-Ala- γ -D-Glu-*m*-DAP-D-Ala-D-Ala) attached to the active site in the SltB3:**4** complex. Final refined ligand is superimposed onto omit map for comparison purposes and is represented as capped sticks colored in yellow for carbon atoms. The proposed catalytic Glu141 is represented as capped sticks and colored in pink for carbon atoms. (B) Refined electron-density map (2Fo-Fc map contoured at 1σ) for the two molecules of compound **4** attached to the active site of the SltB3:**4** complex. Ligand is represented as in panel A. (C) Fo-Fc omit map contoured at 2σ for the two molecules of compound **3** (*N*-acetylglucosamine-1,6-anhydro-*N*-acetylmuramyl L-Ala- γ -D-Glu-*m*-DAP-D-Ala-D-Ala) observed in the SltB3:**3** complex. Final refined modeled ligand is superimposed onto omit map for comparison purposes and is represented as capped sticks colored in blue for carbon atoms. The proposed catalytic Glu141 is represented as capped sticks and colored in pink for carbon atoms. (D) Refined electron-density map (2Fo-Fc map contoured at 1σ) for the two molecules of compound **3** observed in the SltB3:**3** complex. Ligands are represented as in panel C. No electron density was observed for the peptide stems or for the sugar ring at position -1 for the two complexes.

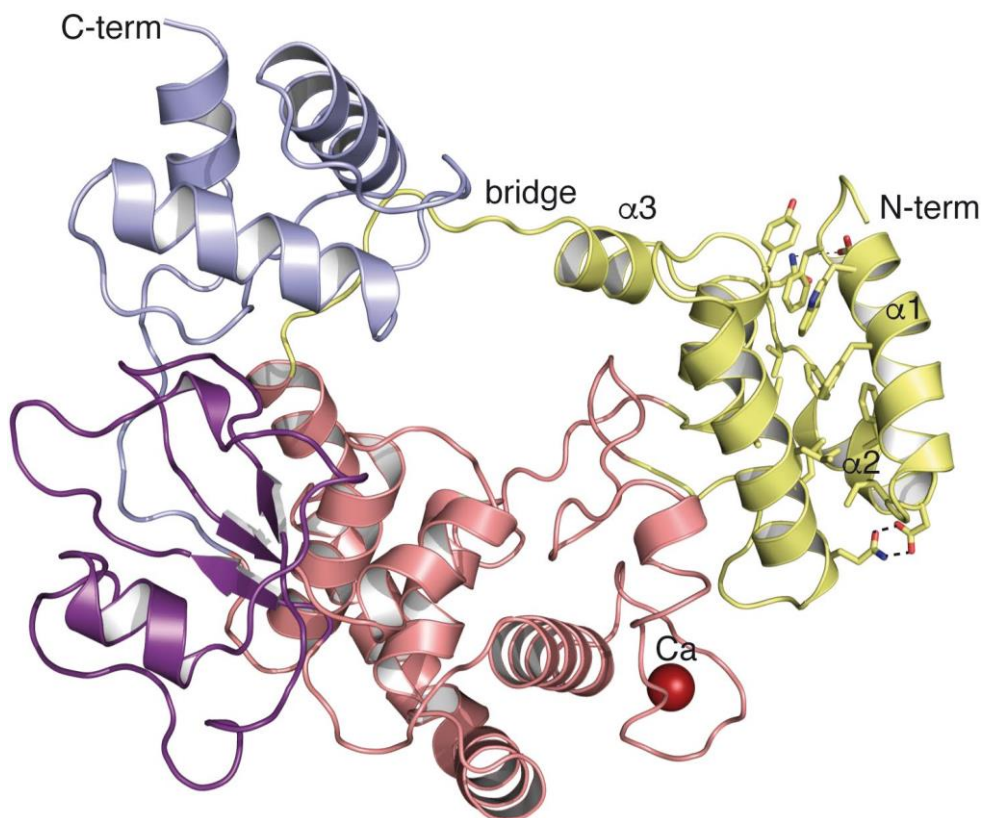


Figure S6. Structural analysis of the interactions found at the core of the N-terminal domain. Many hydrophobic residues and some polar residues (all depicted as capped sticks) comprise the core of the N-terminal domain linking the first three helices with the other two within the domain.

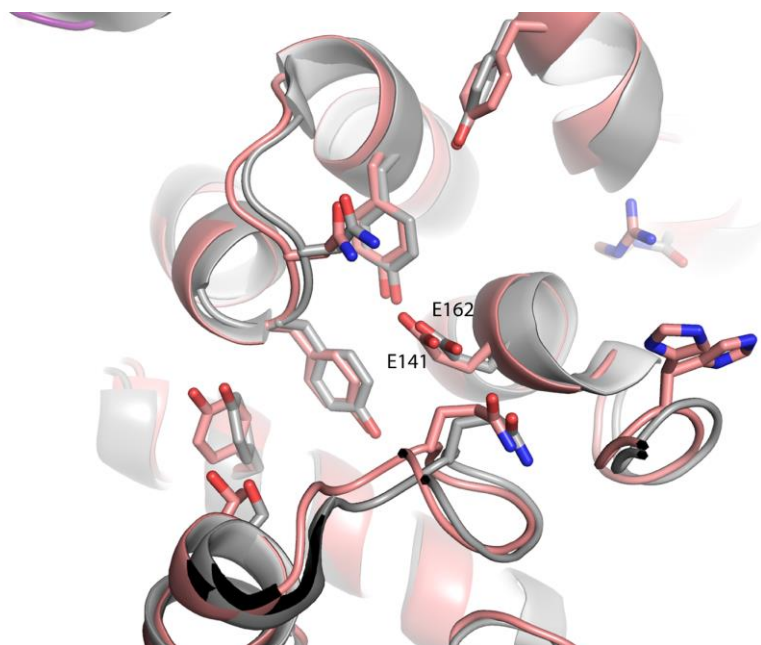


Figure S7. Structural comparison of active sites of SltB3 (pink) and Slt35 from *E. coli* (PDB 1QUS) (grey). Catalytic glutamate residues in both structures are labeled.

References

- (1) Heseck, D., Lee, M., Zhang, W. L., Noll, B. C., and Mobashery, S. (2009) Total synthesis of *N*-acetylglucosamine-1,6-anhydro-*N*-acetylmuramylpentapeptide and evaluation of its turnover by AmpD from *Citrobacter freundii*. *J. Am. Chem. Soc.* *131*, 5187-5193; Lee, M., Heseck, D., Shah, I. M., Oliver, A. G., Dworkin, J., and Mobashery, S. (2010) Synthetic peptidoglycan motifs for germination of bacterial spores. *ChemBioChem* *11*, 2525-2529; Lee, M. J., Zhang, W. L., Heseck, D., Noll, B. C., Boggess, B., and Mobashery, S. (2009) Bacterial AmpD at the crossroads of peptidoglycan recycling and manifestation of antibiotic resistance. *J. Am. Chem. Soc.* *131*, 8742-8743.
- (2) Artola-Recolons, C., Lee, M., Bemardo-Garcia, N., Blazquez, B., Heseck, D., Bartual, S. G., Mahasenan, K. V., Lastochkin, E., Pi, H. L., Boggess, B., Meindl, K., Uson, I., Fisher, J. F., Mobashery, S., and Hermoso, J. A. (2014) Structure and cell wall cleavage by modular lytic transglycosylase MltC of *Escherichia coli*. *ACS Chem. Biol.* *9*, 2058-2066.
- (3) Holm, L., and Rosenström, P. (2010) Dali server: conservation mapping in 3D. *Nucleic Acids Res.* *38*, W545-W549.